ISSN 1392 - 1207. MECHANIKA. 2013 Volume 19(2): 128-134

Experimental and numerical stress analysis of FML plates with cutouts under in-plane loading

Saleh Yazdani*, G. H. Rahimi, Mehdi Ghanbari*****
**Mechanical Engineering Department, Tarbiat Modares University, Tehran, Iran, E-mail: yazdani.saleh@yahoo.com*
***Mechanical Engineering Department, Tarbiat Modares University, Tehran, Iran, E-mail: rahimi_gh@modares.ac.ir*
****Mechanical Engineering Department, Tarbiat Modares University, Tehran, Iran,*
E-mail: mehdi.ghanbari.f@gmail.com

crossref http://dx.doi.org/10.5755/j01.mech.19.2.4152

1. Introduction

The idea of using two materials like aluminium alloys and fiber reinforced composites to have advantages of both materials was raised in two decades ago. Fiber metal laminates (FML) were developed by ALCOA and with commercial brand; ARALL (Aramid Reinforced Aluminium Laminates) had been entered to industry in 1982. GLARE (Glass Laminated Reinforced Aluminum) is the name of the most commonly used FML, in which composite layer is made by glass fibers. Researchers have shown that using Glare structures is more expensive than aluminium in aerospace industry, but due to lightness and high strength of glass fibers, they are widely used [1-4]. It has been done so little works with the FMLs, especially with E-glass woven layers which are used in this paper. Therefore, finding material properties of this kind of FMLs is a critical task. All kinds of FMLs have inelastic behavior because of plasticity response of aluminium layers [5]. Vogelesang et al. [2] introduced fiber metal laminates as appropriate structures in aerospace manufacturing, because of good corrosion resistance, easy manufacturing, and excellent impact resistance. Material properties of special type of FML composites, namely the steel/aluminum/GRP laminates, had been studied by Khalili et al. [6]. G. Reyes and H. Kang [7] have studied tensile and fatigue properties of thermoplastic fiber metal laminates and compared Curve-based and Twintex-based thermoplastic FML's behavior. Also, E.C. Botelho et al. [8] have carried out the influences of temperature and humidity on tensile properties of GLARE laminates, and compared it with non-conditioned ones. The results of this study showed that there is no change in tensile strength of GLARE after forcing hygrothermal condition. So, these structures have good efficiency in aerospace industries. Residual strength of glass fiber metal laminates with notch has been investigated by Guocai Wu et al. [9]. The variations in behavior of any types of FMLs encourage researchers to investigate material properties of all types of them. Experimental and numerical full scale fatigue test of FML panels have been investigated by E. Armentani et al. [10]. In this study, strain gauges had been used and this research is the base idea of our work. Moreover, some investigations have been performed in the field of stress concentration of composite plates with circular hole by Hwai-Chung Wu and Bin Mu [11], or Lotfi Toubal et al. [12], or C. K. Cheung et al. [13], and composite plates with other types of cutouts by D. K. Nageswara Rao [14]. A. Ziliukas*et* al. [15] studied the fracture of layered composite structures contained two aluminium layers and observed that the delamination between layers begins when the specimen is deformed under bending load.

This paper presents experimental and finite element analysis (FEA) of FML plates with cutouts. Circular and elliptical cutouts were considered and the effect of cutout's types on stress concentration and stress field were investigated. Global mechanical properties of FML with E-glass woven layers were not available. Therefore, the global material properties were carried out by the simple tension tests. Strain gauges were used to measure the strain values near the cutout and then stresses were estimated. Finally, results of two methods were compared.

2. Experimental procedures

The rectangular plates with dimension of length a = 104 mm, width b = 100 mm, and average thicknesses t_1 = 1.4 mm for one of them, and t_2 = 1.7 mm for the other one were manufactured. The diameters of the two circular cutouts were $d_1 = d_2 = 7$ mm and $d_1 = d_2 = 14$ mm. Two types of elliptical cutouts were considered. Major and minor diameters of which were d_1 = 28 mm and d_2 = 14 mm, respectively. In one of them major diameter was aligned in load direction (elliptical cutout 1) and in the other one minor diameter was aligned in this direction (elliptical cutout 2). Fig. 1 shows the schematic view of plate's dimensions.

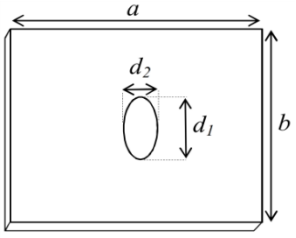

Fig. 1 Schematic view of plate's dimension

Each specimen contains 5 plies, 3 layers of aluminium alloy 2024-t3 and two fabricated glass woven layers. Resin type was cy219 and was used as interlayer to bond the sheets to each other. The thicknesses of aluminium layers were 0.3 mm and 0.4 mm, and of the woven layers was 0.2 mm. The average thickness of plates was 1.4 mm and 1.7 mm. The reason of this difference between thicknesses of these sheets is to investigate the effects of aluminium on stress distributions. Lay-up method was used and material properties of each individual layer are

shown in Table 1. In order to prevent delamination of plates, waterjet was used for creating cutouts.

Table 1
Material properties of woven and aluminium [16]

Al	E, GPa		v	
	71.1		0.33	
Woven/	E_L, GPa	E_T, GPa	G_{LT}, GPa	v_{LT}
Glass epoxy	15.8	15.8	2.8	0.25

where E and v are the material properties of aluminium layers; and E_T, E_L are Young moduli in principal directions, G_{LT} is shear modulus, and v_{12} is Poisson's ratio of composite layers. The schematic view of stacking sequence is shown in Fig. 2.

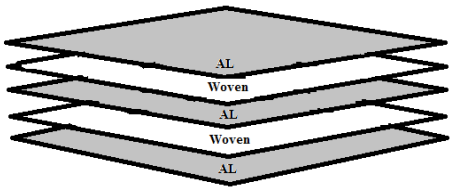

Fig. 2 Schematic view of FML lay-up

2.1. Evaluation of material properties

In order to find tensile modulus of the FML plates, standard dog bone samples were tested in an Instron 5500 machine with a capacity of 200 kN. Tensile tests were carried out using eight samples which were produced by cutting initial plates with waterjet machine. Fig. 3 and Fig. 4 show the experimental tensile test and the samples which were used, respectively.

Fig. 3 Tensile test for finding material properties

As it can be seen in Fig. 4, standard samples were performed in two directions, 0° and 45°, and by using Eq. (1), G_{12} can be easily calculated. In this work we considered the FML plates as one orthotropic layer plate to obtain global mechanical properties of them and using them in FEA. This helped us to reach to close results by comparing the two methods. The amount of v_{12} was used from Botelho's work [4].

$$\frac{1}{E_x}=\frac{1}{E_1}cos^4\theta+\left[\frac{1}{G_{12}}-\frac{2v_{12}}{E_1}\right]sin^2\theta\,cos^2\theta+\frac{1}{E_2}sin^4\theta\,, \quad (1)$$

where E_x is the Young's modulus in x direction, E_1, E_2, G_{12}, v_{12} are material properties in principal direction, and θ is the angle between these two directions.

Fig. 4 Standard samples for tensile tests

2.2. Testing procedure

All the plates with different types of cutouts were subjected to in-plane loading. The test was carried out by an Instron 5500 machine with a loading rate of 1.3 mm/min which provides static loading conditions (Fig. 5).

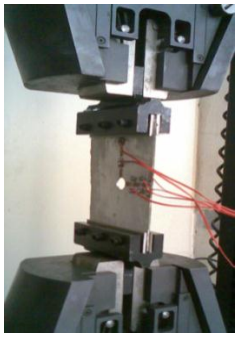

Fig. 5 Experimental model: FML plate with cutout

Plates have been tested to determine stress distribution in special amount of loading (here 6 kN considered). Some of the tools which are widely used for measuring the strain are strain gauges. S. J. Guo [17] used this method for obtaining stress concentration in composite panels. Also, K. Rasiulis et al. [18] used it to obtain stress concentration in steel plate with geometrical defect. Therefore, in experimental works the amount of strains by using strain gauges were obtained. To record the amount of strain gauge measurements, DATA logger device was used. Strain gauges were attached in two principal directions because of lack of shear strains in our in-plane loading conditions. Fig. 6 shows the positions and directions of strain gauges.

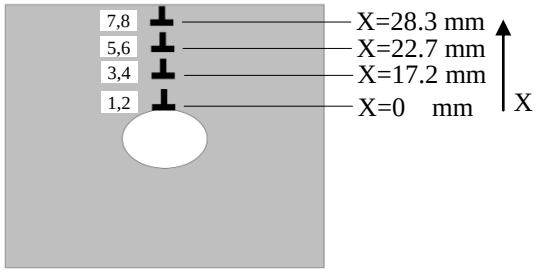

Fig. 6 Positions and directions of strain gauges

To measure the precise values of strain, the DATA logger device was calibrated. Longitudinal strains of standard steel specimens were measured with extensometer and were compared with longitudinal strain gauge values reported by DATA logger (Fig. 7).

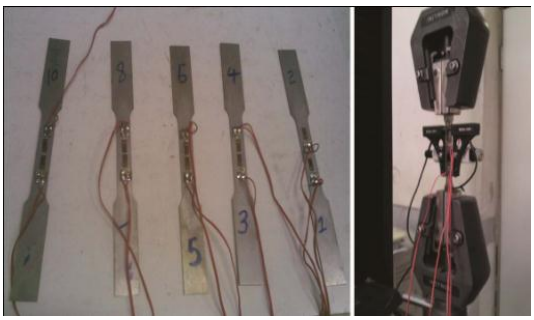

Fig. 7 Calibrating the DATA logger device

Finally, the changes were performed in the equation in the device program to obtain the precise values of strain. Experimental results are given in section 4.

3. Finite element analysis

Numerical simulations have been carried out using the general purpose of finite element program ABAQUS 6.9-3 standard. In order to comparison, dimensions used in modeling the plates in ABAQUS were the same as the experimental work. One quarter of the laminates was modeled because of the symmetry of the geometry, loading, and boundary conditions.

3.1. Mesh, loading, and boundary conditions

The points along the x axis were constrained in the y direction and the points along the y axis were constrained along x direction. At the edges where plates were subjected to loading, all degrees of freedom were removed, except the displacement in x direction. Plate is subjected to in-plane tensile loading F = 6 kN. Fig. 8 shows the boundary conditions and loading.

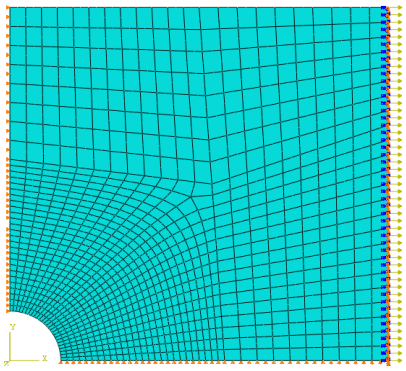

Fig. 8 FE model meshing and boundary conditions

The model has been meshed with parabolic thick shell elements (S8R), because this type of element is allowed to have a linear variation of stress across the element, and through thickness stresses to be modeled. Several different finite-element models with different levels of mesh refinement have been developed. Arrangement and type of element scheme changed several times to achieve convergent results, and then accurate results were selected. Finite element mesh is shown in Fig. 8.

3.2. Analysis

Generally, static method has been employed for FEA. This analysis was performed for plate in one orthotropic ply, and global mechanical properties of lamina that are presented in Table 2 are used. Fig. 9 shows Von-Mises stress distributions in plates after subjecting to the same tensional in-plane loading (here 6 kN considered).

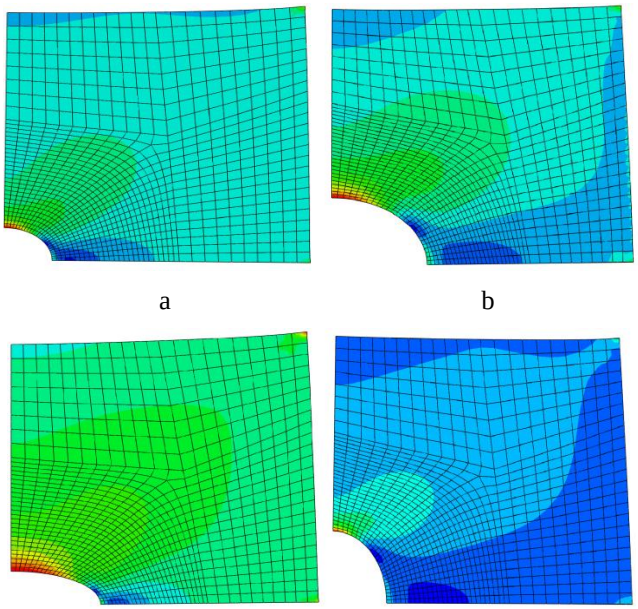

Fig. 9 Von-Mises stress distribution in the laminates: a) small circular cutout; b) big circular cutout; c) elliptical cutout 1; d) elliptical cutout 2

According to Fig. 9, it is obvious that how much the type of cutout is important in changing the amount of stress distributions and stress concentrations in a laminate.

4. Results and discussion

Tensile properties of FML were investigated using dog-bone samples. Stress-strain for samples with thicknesses 1.4 mm and 1.7 mm, are shown in Fig. 10 and Fig. 11, respectively.

According to the Fig. 10, Fig. 11 and the Eq. (1), the measurements of mechanical properties for both samples, with thicknesses 1.4 mm and 1.7 mm separately, were obtained and represented in Table 2.

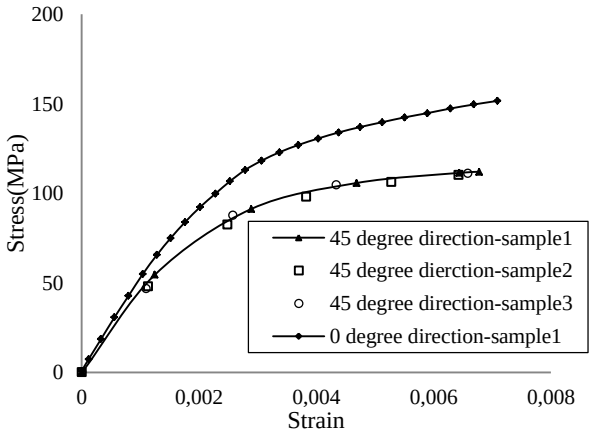

Fig. 10 Engineering tensile stress-strain curves for samples with thickness 1.4 mm

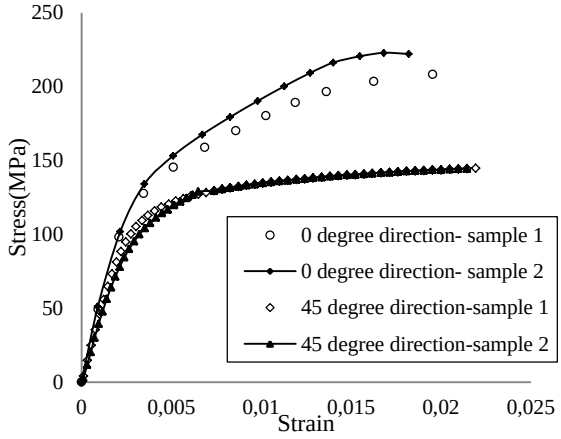

Fig. 11 Engineering tensile stress-strain curves for samples with thickness 1.7 mm

Table 2
Measurement of the global mechanical properties

Plate thickness	E_0, GPa	E_{45}, GPa	G_{12}, GPa
1.4 mm	51.93	42.362	15.25
1.7 mm	52.83	43.47	15.717

where E_0 and E_{45} are the laminate's global extensional moduli in 0° and 45° directions, and G_{12} is global shear modulus obtained by using these moduli and Eq. (1). By comparing the trend of samples with 1.4 mm and 1.7 mm thicknesses it can be concluded that the samples with more aluminium thickness have higher modulus and yield stress. Also, aluminium helps FML samples to show better behavior in elastic region. By comparing Fig. 10 and Fig. 11 the values of strain in elastic region in samples with 1.7 mm thickness are more than samples with 1.4 mm thickness. It is attributed to their more volume ratio of aluminium to composite. Furthermore, it makes thicker samples show more flexible behaviors than thinner ones under their plastic instability loads in non-linear regions. Stress-strain relations in composite materials were used, to calculate stresses through amount of strains obtained from plates tension tests, and are shown in Eq. (2) to Eq. (6) [19]:

$$\begin{bmatrix}\sigma_1\\ \sigma_2\\ \tau_{12}\end{bmatrix}=\begin{bmatrix}Q_{11} & Q_{12} & 0\\ Q_{12} & Q_{22} & 0\\ 0 & 0 & Q_{66}\end{bmatrix}\begin{bmatrix}\varepsilon_1\\ \varepsilon_2\\ \gamma_{12}\end{bmatrix}; \tag{2}$$

$$Q_{11}=\frac{E_1}{1-\upsilon_{12}\upsilon_{21}}; \tag{3}$$

$$Q_{22}=\frac{E_2}{1-\upsilon_{12}\upsilon_{21}}; \tag{4}$$

$$Q_{12}=Q_{21}=\frac{\upsilon_{12}E_2}{1-\upsilon_{12}\upsilon_{21}}; \tag{5}$$

$$Q_{66}=G_{12}, \tag{6}$$

where Q represent the reduced stiffness matrix for plane stress state in 1-2 plane (principal directions); $E_1 = E_2 = E_0$ are Young's modulus; $v_{12} = v_{21} = 0.25$ are Poisson's ratio in 1-2 plane. The global mechanical properties obtained from experimental tension tests, presented in Table 2, were used in the calculations of reduced stiffness matrix's components.

In the tension tests of all plates, the strain values for all loadings were reported to ensure that the behaviors of the strains are linear, and consequently, the results presented to analyze the stress of the plates are in elastic range. All measurements of tension tests were calculated under loading 6 kN. The predictions of stress distribution using the finite element method are compared to the experimental data in Figs. 12-19.

The results of two methods have close stress values. It shows that by using global mechanical properties and considering the plate as one orthotropic layer, instead of the ply by ply mechanical properties in modeling, the results in finite element modeling can be close to the

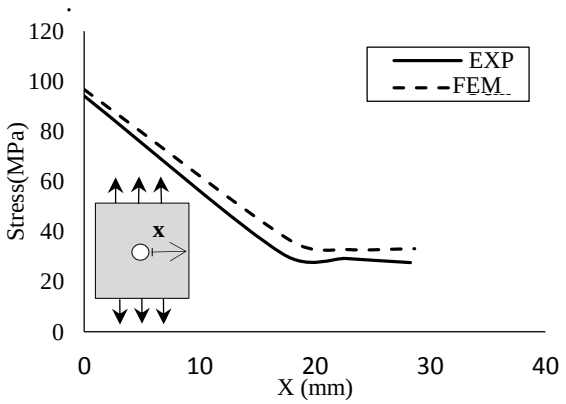

Fig. 12 Stress distribution in plate with 1.4 mm thickness and small circular cutout

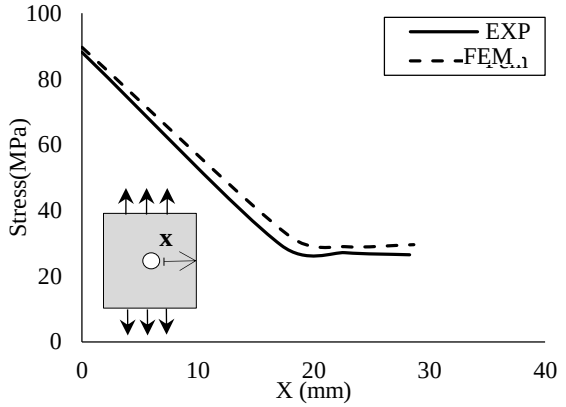

Fig. 13 Stress distribution in plate with 1.7 mm thickness and small circular cutout

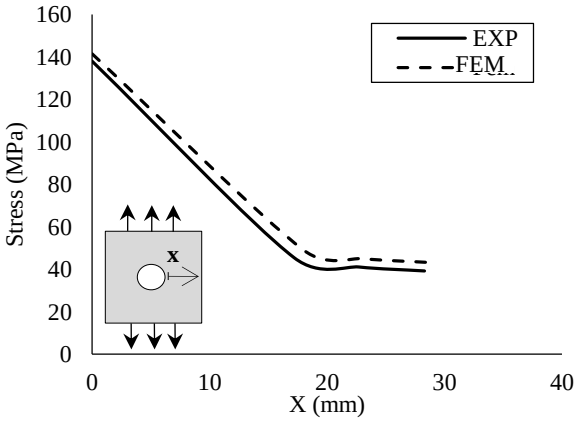

Fig. 14 Stress distribution in plate with 1.4 mm thickness and big circular cutout

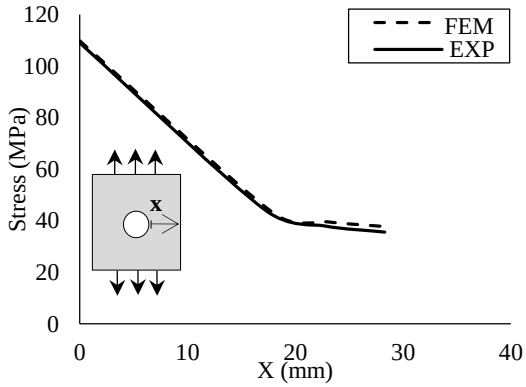

Fig. 15 Stress distribution in plate with 1.7 mm thickness and big circular cutout

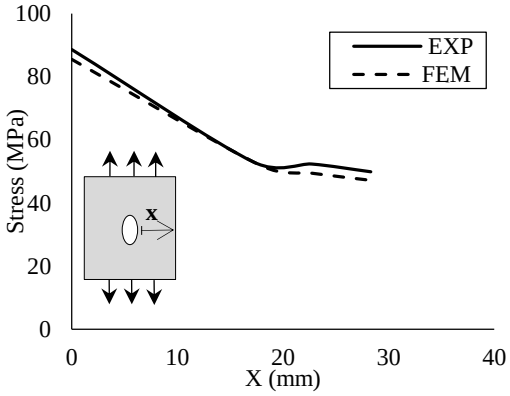

Fig. 16 Stress distribution in plate with 1.4 mm thickness and elliptical cutout 1

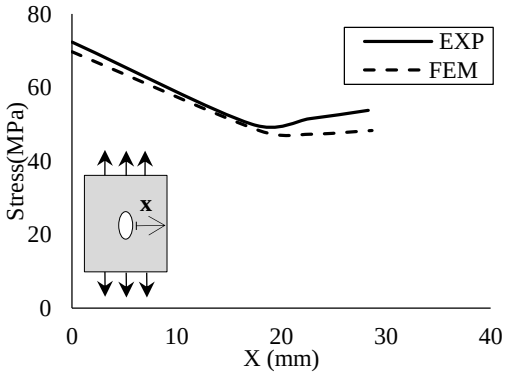

Fig. 17 Stress distribution in plate with 1.7 mm thickness and elliptical cutout 1

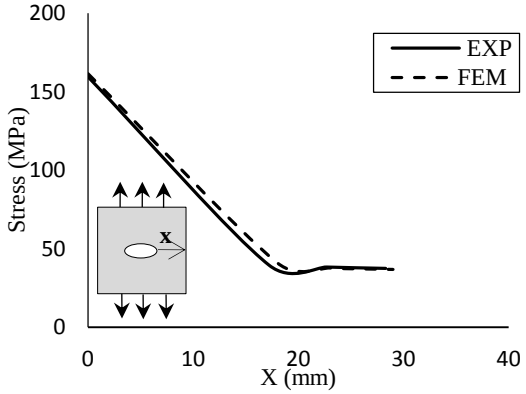

Fig. 18 Stress distribution in plate with 1.4 mm thickness and elliptical cutout 2

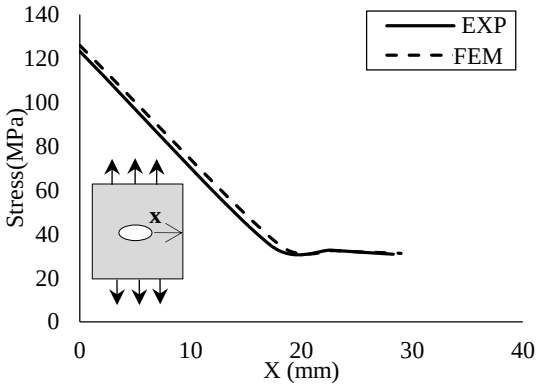

Fig. 19 Stress distribution in plate with 1.7 mm thickness and elliptical cutout 2

experimental results. Moreover, stress values were obtained in elastic region that the delamination in layers did not observe in it. Therefore, it makes to have close results in two methods, too. In all graphs, the stresses have high values around the cutout and by reaching to the plates' edge they are decreased and tend to constant values. The maximum stress value near the cutout, is related to the plate with elliptical cutout 2, in which the minor diameter of the ellipse was aligned in load direction, and the minimum value is for the elliptical cutout 1, in which major diameter was aligned in load direction.

By comparing the stress values in plates with different circular cutout radius, Figs. 12 and 14, it is obvious that by increasing the cutout's size while not changing its type the amount of stress around the cutout's edge was increased. Moreover, by comparing Fig. 12 with Fig. 13, and also, Fig. 14 with Fig. 15, it can be concluded that stress values were decreased around the cutout's edge in the thicker plates. This fact is also agreed in plates with elliptical cutout by comparing Fig. 16 with Fig. 17 and Fig. 18 with Fig. 19. Stress values near the cutout's edge for elliptical cutout 2 in Fig. 18 and Fig. 19 were too much and they decreased suddenly by getting close to the plate's edge.

The exact solution of the stress distribution of an infinite orthotropic composite laminate with an elliptical cutout present by Lekhnitskii [20]:

$$\sigma_y(x,0) = \overline{\sigma_y} \times \left\{ Re\frac{1}{\mu_1-\mu_2} \times \left[\frac{-\mu_2\left(1-i\mu_1\lambda\right)}{\sqrt{\gamma^2-1-\mu_1^2\lambda^2}\left(\gamma+\sqrt{\gamma^2-1-\mu_1^2\lambda^2}\right)} + \frac{\mu_1\left(1-i\mu_2\lambda\right)}{\sqrt{\gamma^2-1-\mu_2^2\lambda^2}\left(\gamma+\sqrt{\gamma^2-1-\mu_2^2\lambda^2}\right)} \right] \right\} + \overline{\sigma_y}, \quad (7)$$

where $\lambda = b/a$, $\gamma = x/a$, and $\overline{\sigma_y}$ is the stress applied at infinity. By considering $x = a$, stress concentration factor (SCF) can be obtained from Eq. (7) as:

$$K_T^{\infty} = 1 + \frac{a}{b}\sqrt{2\left(\sqrt{\frac{E_y}{E_x}} - \nu_{yx}\right) + \frac{E_y}{G_{xy}}}, \quad (8)$$

where K_T^{∞} is stress concentration factor; E_x, E_y and G_{xy} are the laminate extensional and shear moduli, respectively, v_{xy} denotes the effective laminate Poisson's ratio; a and b are the elliptical cutout's radius.

In Eq. (8), by considering $a = b$, the SCF for orthotropic plate with circular cutout can be achieved as:

$$K_T^{\infty} = 1 + \sqrt{2\left(\sqrt{\frac{E_y}{E_x}} - v_{yx}\right) + \frac{E_y}{G_{xy}}}. \quad (9)$$

By comparing stress values near cutout in Fig. 12 with Fig. 14, and also Fig. 13 with Fig. 15, by increasing the size of cutout stress concentration was significantly increased. This is in opposition with Lekhnitskii's equation, because according to the Eq. (9), the increment in size of cutout has no effect on the values of stress concentration and K_T^{∞} only depends on the material properties of plate.

By comparing the measures of stress in plates with thicknesses of 1.4 mm and 1.7 mm, it could also observe that the increment of thickness (which here is merely related to the aluminium sheets) is effective in value of stress distribution. This fact is completely obvious also in decrement of the stress concentration. Moreover, it shows that the role of the thickness of the plate and using aluminium with a few more thickness is significant. It causes to have better behavior in elastic region and less stress distribution in FMLs. Therefore, the effect of aluminium in decreasing the damage in plates (especially with cutouts) is high. The measurements of SCF for plates with different types of cutouts are given in Table 3.

Table 3

The measurements of stress concentration factor (SCF) for plates with different types of cutouts

Thickness	Method	Cutout type			
		Small circular	Big circular	Elliptical 1	Elliptical 2
1.4 mm	Experiment	3.41	3.52	1.77	4.25
	Finite element	2.94	3.28	1.816	4.37
	Lekhnitskii	3.2147		2.1073	5.4295
1.7 mm	Experiment	3.32	3.45	1.34	4
	Finite element	2.67	2.92	1.47	4.04
	Lekhnitskii	3.2048		2.1024	5.4096

As it is clear in Table 3, the maximum measurements of stress concentration are related to the elliptical cutout 2 and the minimum is related to elliptical cutout 1. The results of finite element method are almost close to the experiments. Lekhnitskii's approach for plates with circular cutout is close to the smaller cutout. However, Lekhnitskii's approach for elliptical cutout has a different response from two other methods. Moreover, the value of stress concentration factor for the thicker plates is less than thinner plates.

5. Conclusion

The experimental and finite element analyses of FML plates containing an elliptical and circular cutout with different thicknesses are presented. Strain gauges were used to measure the strain values near the cutout, and then stresses were computed in the linear range. Stress distributions in experimental and numerical results have shown good agreement. Standard tensile results of samples with 1.7 mm thicknesses obtained in stress-strain diagrams showed more flexible behavior in elastic region than samples with 1.4 mm, and aluminium helps FMLs to show better behavior in elastic region and provides plates' nonlinear deformation under their plastic instability loads. It is shown that using global mechanical properties instead of the ply by ply mechanical properties in modeling are quite accurate. Although in Lekhnitskii's approach the SCF only depends on material properties of the laminate, the experimental and finite element results on SCF of the plates with circular cutout revealed the significant effect of the cutout's aspect ratio in SCF's value. We also observed that the stress gradient and SCF in FMLs with thicker aluminium layers is less than thinner ones.

References

1. **Vlot, A.; Gunnink, J.W.** 2001. Fibre metal laminates, Kluwer Academic, Netherlands, 3-31 p.
2. **Vogelesang, L.B.; Vlot, A.** 2000. Development of fibre metal laminates for advanced aerospace structures, J. Mater. Process. Technol. 103(1): 1-5. http://dx.doi.org/10.1016/S0924-0136(00)00411-8.
3. **Van Rooijen, R.; Sinke, J.; De Vries, T.J.; Van Der Zwaag, S.** 2004. Property optimization in fibre metal laminates, Appl. Compos. Mater. 11(2): 63-76. http://dx.doi.org/10.1023/B:ACMA.0000012880.01669.c0.
4. **Botelho, E.C.; Pardini, L.C.; Rezende, M.C.** 2005. Hygrothermal effects on damping behavior of metal/glass fiber/epoxy hybrid composites, Materials Science and Engineering A 399: 190-198. http://dx.doi.org/10.1016/j.msea.2005.02.093.
5. **Guocai Wu; Yang, J-M.** 2005. The mechanical behavior of GLARE laminates for aircraft structures, Failure in Structural Materials 57(1): 72-79.
6. **Khalili, S.M.R.; Mittal, R.K.; S. Gharibi Kalibar.** 2005. A study of the mechanical properties of steel/aluminium/GRP laminates, Materials Science and Engineering A 412: 137-140. http://dx.doi.org/10.1016/j.msea.2005.08.016.
7. **Reyes, G.; Kang, H.** 2007. Mechanical behavior of lightweight thermoplastic fiber-metal laminates, J of Materials Processing Technology 186(1-3): 284-290. http://dx.doi.org/10.1016/j.jmatprotec.2006.12.050.
8. **Botelho, E.C.; Almeida, R.S.; Pardini, L.C.; Rezen-**

de, M.C. 2007. Elastic properties of hygrothermally conditioned glare laminate, Int. J. of Engineering Science 45(1): 163-172. http://dx.doi.org/10.1016/j.ijengsci.2006.08.017.
9. **Guocai Wu; Yi Tan; Jenn-Ming Yang**. 2007. Evaluation of residual strength of notched fiber metal laminates, Materials Science and Engineering A 457: 338-349. http://dx.doi.org/10.1016/j.msea.2006.12.135.
10. **Armentani, E.; Citarella, R.; Sepe, R.** 2011. FML full scale aeronautic panel under multiaxial fatigue: Experimental test and DBEM Simulation, Engineering Fracture Mechanics 78(8): 1717-1728. http://dx.doi.org/10.1016/j.engfracmech.2011.02.020.
11. **Hwai-Chung Wu; Bin Mu.** 2003. On stress concentration for isotropic/orthotropic plates and cylinders with circular hole, Composites: Part B 34(2): 127-134. http://dx.doi.org/10.1016/S1359-8368(02)00097-5.
12. **Lofti Toubal; Moussa Karama; Bernard Lorrain** 2005. Stress concentration in a circular hole in composite plate, Composite Structures 68(1): 31-36. http://dx.doi.org/10.1016/j.compstruct.2004.02.016.
13. **Cheung, C.K.; Liaw, B.M.; Delale, F.** 2004. Composite strips with a circular stress concentration under tension, International Congress & Exposition on Experimental and Applied Mechanics Costa Mesa, CA, June 7-10.
14. **Nageswara Rao, D.K.; Ramesh Babu, M.; Raja Narender Reddy, K.; Sunil, D.** 2010. Stress around square and rectangular cutouts in symmetric laminates, Composite Structures 92(12): 2845-2859. http://dx.doi.org/10.1016/j.compstruct.2010.04.010.
15. **Žiliukas, A.; Meslinas, N.; Juzėnas, K.** 2006. Fracture investigation of layered composite structural elements. Mechanika 1(57): 12-16.
16. **Golzar, M.; Poorzeinolabedin, M.** 2010. Prototype fabrication of a composite automobile body based on integrated structure, Int. J. Adv. Manuf. Technol. 49: 1037-1045. http://dx.doi.org/10.1007/s00170-009-2452-6.
17. **Guo, S.J.** 2007. Stress concentration and buckling behavior of shear loaded composite panels with reinforced cutouts, Composite Structures 80(1): 1-9. http://dx.doi.org/10.1016/j.compstruct.2006.02.034.
18. **Rasiulis, K.; Samofalov, M.; Šapalas, A.** 2006. Stress and strain state investigation of soft defects on thin steel plate using experimental and numerical methods, Mechanika 3(59): 19-27.
19. **Jones, R.M.** 1999. Mechanics of Composite Materials, New York, Taylor & Franics, 519 p.
20. **Lekhnitskii, S.G.; Tsai, S.W.; Cheron, T.** 1968. Anisotropic Plates, New York: Gordon and Breach Science Publishers, 534 p.

Saleh Yazdani, G. H. Rahimi, Mehdi Ghanbari

EKSPERIMENTINĖ IR SKAITINĖ PML PLOKŠTELIŲ SU IŠPJOVOMIS ĮTEMPIŲ ANALIZĖ, KAI JŲ PLOKŠTUMA YRA APKRAUTA

R e z i u m ė

Straipsnyje pateikta pluošto, metalo ir laminato (PML) plokštelių su skirtingos formos išpjovomis įtempių eksperimentinė ir skaitinė analizė. PML susideda iš metalo, šiuo atveju aliuminio, lakštų, sustiprintų epoksidinės dervos pluoštu. Mechaninės PML savybės nustatytos standartiniais tempimo bandymais. Deformacijoms šalia išpjovų matuoti buvo panaudoti deformacijų jutikliai. Įtempiai nustatyti atsižvelgiant į mechanines savybes, nustatytas eksperimento metu. Be to, antrajame etape buvo atlikta baigtinių elementų analizė. Galiausiai buvo palyginti eksperimentiniai ir skaitinės analizės rezultatai.

Saleh Yazdani, G. H. Rahimi, Mehdi Ghanbari

EXPERIMENTAL AND NUMERICAL STRESS ANALYSIS OF FML PLATES WITH CUTOUTS UNDER IN-PLANE LOADING

S u m ma r y

In the present study, the experimental and numerical stress analysis of Fiber Metal Laminates (FML) with different types of cutouts was investigated. FMLs consist of combination of metal sheets, especially aluminium ones, with fiber reinforced epoxy layers. Mechanical properties of FML were investigated by standard tensile tests. Strain gauges were used to measure the strain values near the cutout and then stresses were estimated according to the mechanical properties which obtained in the experiments. Moreover, finite element analysis was applied as the second method. Finally, experimental and finite element results were compared.

Keywords: FML, cutout, stress analysis, SCF, finite element.

Received October 26, 2011
Accepted March 04, 2013